Regulation of Intracellular pH in Human Melanoma: Potential Therapeutic Implications[1]

Miriam L. Wahl,[2] Judith A. Owen, Randy Burd, Robin A. Herlands, Suzanne S. Nogami, Ulrich Rodeck, David Berd, Dennis B. Leeper, and Charles S. Owen

Department of Biochemistry and Molecular Pharmacology [M. L. W., C. S. O.], and Department of Biology [J. A. O., R. A. H., S. S. N.], Haverford College, Haverford, Pennsylvania 19041, and Departments of Radiation Oncology [R. B., D. B. L.], Dermatology and Cutaneous Biology [U. R.], and Medicine [D. B.], and Kimmel Cancer Center [M. L. W., D. B. L.], Thomas Jefferson University, Philadelphia, Pennsylvania 19107

Abstract

Melanoma cells *in vivo* maintain intracellular pH (pH_i) in a viable range despite an extracellular tumor pH (pH_e) that is typically below 7.0. In general, three families of transporters are capable of removing metabolic protons, but the specific transporters responsible for the maintenance of pH_i at low pH_e in melanomas have not been identified. Although the transporters exist in most cells, an inhibitor would be predicted to have selectivity for cells located in an acidic tumor bed because cells in that environment would be expected to have transporters chronically activated. In this report, the levels and extent of expression of the Na^+/H^+ exchanger (NHE-1) and two of the H^+-linked monocarboxylate transporters (MCTs) were evaluated in three melanoma cell lines. The effects of inhibitors of each transporter were tested at an extracellular pH (pH_e) of 7.3, 6.7, or 6.5 in melanoma cells that were grown at pH_e 7.3 or 6.7. The activity of MCT isoform 1 (MCT-1) was up-regulated in three melanoma cell lines at low pH_e, but that of NHE-1 was not. Furthermore, NHE-1 activity was lower in the melanomas than in other normal and malignant cell lines that were tested. Reverse transcription-PCR using primers specific for MCT-1, MCT-4, and NHE-1 showed that expression of none of these transporters was reproducibly up-regulated at the level of transcription when cells were grown at pH_e 6.7 instead of pH_e 7.3. *Ex vivo* experiments using DB-1 human melanoma xenografts grown in severe combined immunodeficient mice found that MCT-1 and not NHE-1 was a major determinant of DB-1 tumor cell pH_i. Taken together, the data indicate that MCTs are major determinants of pH regulation in melanoma. In contrast, keratinocytes and melanocytes under low pH_e conditions relied on NHE-1. Inhibitors of MCTs thus have great potential to improve the effectiveness of chemotherapeutic drugs that work best at low pH_i, such as alkylating agents and platinum-containing compounds, and they should be selective for cells in an acidic tumor bed. In most tissues, it is proposed that the NHE-1 could compensate for an inhibited MCT to prevent acidification, but in melanoma cells this did not occur. Therefore, MCT inhibitors may be particularly effective against malignant melanoma.

Introduction

Many cellular processes, such as enzyme activity, macromolecular synthesis, transport of metabolites, and cell cycle progression, are dependent on the maintenance of pH_i[3] in the physiological range. In tumors, despite an pH_e of 5.6–7.6, the pH_i is typically in the normal range of 6.9–7.4 (1). There has been interest in recent years in potentiating tumor therapy by compromising cellular pH_i control using inhibitors of ion transport (2–5).

We have evaluated three classes of transporters used by the cell to regulate pH_i. The NHE is found in most cell types that have been studied (6–10), including human melanoma cells (11). NHE-1 activity was evaluated in the present study with the inhibitor cariporide mesilate (HOE642) (12). The activity of the Na^+-dependent Cl^-/HCO_3^- exchanger was investigated with the inhibitor DIDS (13, 14). MCTs, which transport lactate or pyruvate together with a H^+ in the same direction (symport), were also evaluated. MCT-1 is the most prevalent of these in tissues, especially in heart and red muscle, and is up-regulated by increased work (15). MCT-4 has been shown to be up-regulated in tissues that have a high glycolytic rate, such as white muscle fibers (16, 17). In the present study, the relative contribution of MCT-1 to pH_i regulation was evaluated, using CNCn or DBDS (18, 19). Characteristics of these inhibitors and transporters are summarized in Table 1.

Received 1/3/02; revised 3/20/02; accepted 5/2/02.
[1] Supported by NIH Grant P01 CA56690 (to M. L. W., R. B., C. S. O., D. B. L.); Grant R25CA48010 from National Cancer Institute, NIH, and Department of Health and Human Services, National Science Foundation MCB RUI Grant 9057010 (to J. A. O., S. S. N., R. A. H.); and NIH Grant CA39248 (to D. B.).
[2] To whom requests for reprints should be addressed, at Department of Biochemistry and Molecular Pharmacology, Thomas Jefferson University, 233 South 10th Street, Room 226, Philadelphia, PA 19107. Phone: (215) 503-7867; Fax: (215) 923-9162; E-mail: Miriam.Wahl@mail.tju.edu.

[3] The abbreviations used are: pH_i, intracellular pH; pH_e, extracellular tumor pH; CNCn, α-cyano-4-hydroxycinnamate; BCECF, bis-carboxyethyl-carboxyl-fluorescein; C.SNARF, carboxy-semi-naphthyl-rhodofluor; DBDS, 4,4′-dibenz-amidostilbene-2,2′-disulfonic acid; DIDS, 4,4′-diisothiocyanato-stilbene-2,2′-disulfonic acid; HMVEC, human microvascular endothelial cell; HUVEC, human umbilical vein endothelial cell; MCT, H^+-linked monocarboxylate transporter; NHE, Na^+/H^+ exchanger (sodium-proton exchanger); NHEM, normal human epidermal melanocyte; RT-PCR, reverse transcription-PCR; SCID, severe combined immunodeficiency/immunodeficient; AM, acetoxymethyl ester; RGD, arginine-glycine-aspartic acid; CCD, charge-coupled device; FACS, fluorescence-activated cell sorting; GAPDH, glyceraldehyde-3-phosphate dehydrogenase.

Table 1 Summary of inhibitors of ion transport used in the present study

Inhibitor	Target	Notes	References
CNCn	MCT-1, MCT-4	Reduces pH_i *in vitro*	(16, 18, 38, 58, 59)
DBDS	MCT-1, MCT-4	Binds irreversibly, is a DIDS analogue, no data *in vivo*	(59)
DIDS	Cl^-/HCO_3^- exchanger at 0.2 mM: has been reported to inhibit MCT-1, MCT-4 at 2 mM	Binds irreversibly to the Cl^-/HCO_3^- exchanger	(13, 14)
Cariporide mesilate (HOE642)	NHE-1	Water soluble	(12)

In common with most cell lines that have been tested, the three melanoma lines showed very little sensitivity to any inhibitor of proton translocation when they were tested in a medium of pH_e 7.3. Under conditions of extracellular acidification, however, all three showed a distinctive and striking dependence on the MCT-1 transporter. The importance of this MCT to melanoma cell maintenance of pH_i was confirmed by observations that melanoma cells that were grown under conditions of chronic acidification (pH_e 6.7) were even more dependent on MCTs. In most cases, they exhibited an up-regulation of one or more isoforms of MCT at the protein level. Melanoma cells exhibited little NHE-1 activity and no up-regulation at pH_e 6.7. In contrast, keratinocytes, frequently the cell type surrounding a melanoma *in situ*, had relatively higher NHE-1 and less MCT activity. Taken together, these results suggest that inhibitors of MCT activity may be useful adjuncts to melanoma therapy, and may be particularly active in tumor populations in which the pH_e is lowest, typically areas that are most refractory to treatment.

Materials and Methods

Reagents. The fluorochromes C.SNARF-1-AM and BCECF-AM and the detergent Pluronic F127 were obtained from Molecular Probes (Eugene, OR). Cariporide mesilate was the generous gift of Dr. Udo Albus (Hoechst AG, Cardiovascular Research, Frankfurt/Mainz, Germany). Type I rat tail collagen was obtained from Collaborative Biomedical Products (Bedford, MA). Fibronectin-like engineered protein polymer and all other reagents were obtained from Sigma Chemical Co. (St. Louis, MO) unless otherwise noted.

Cell Culture. The Sk-Mel-28 human melanoma cell line was obtained from the American Type Culture Collection (Rockville, MD). DB-1 and DB-8 melanoma cells were early passage human melanoma cells derived from lymph node biopsies from metastatic patients and were provided by Dr. David Berd (Thomas Jefferson University Hospital, Philadelphia, PA). All of these cell lines were maintained in logarithmic growth at 37°C as monolayers in 75-cm^2 flasks. The melanoma cells were grown in α-modified Eagle's medium (αMEM) containing 12 mM glucose, 2 mM nonessential amino acids, 2 mM glutamine, and 10% heat-inactivated fetal bovine serum (complete medium). This medium had a bicarbonate concentration of 26 mM, and it provided a pH_e of 7.3 under 5% CO_2 and a pH_e 6.7 under 17% CO_2. Cells were subcultured every 7 days by trypsinization. The pH of the medium was stable over this time interval and was monitored regularly. Sk-Mel-28 cells had a doubling time of 72 h, and the DB-1 and DB-8 cells had doubling times of 48 h. These doubling times were unchanged by growth at low pH_e when achieved, as in the present study, by raising the CO_2 from 5% to 17% rather than reducing the bicarbonate in the medium. HaCaT cells, which are immortalized nontumorigenic keratinocytes, were provided by Norbert Fusenig (DKFZ, Heidelberg, Germany) and were grown in Madin-Darby canine kidney (MDCK) medium as described previously (20). Primary NHEMs were cultured by Dr. Ulrich Rodeck (Department of Dermatology, Thomas Jefferson University) as described previously (21). Experiments with melanocytes and HaCaT cells were performed in medium devoid of growth factors. HMT3522-T4/2 malignant breast cells were provided by Per Briand (The Danish Cancer Society, Copenhagen, Denmark), and were maintained as described previously (5). PS120 cells, which overexpress NHE-1 protein (22), were provided by Diane Barber (University of California-San Francisco, San Francisco, CA) with kind permission from Jacques Pouyssegur (University of Nice, Nice, France).

HUVECs were obtained from umbilical cord blood made available from the maternity ward of Thomas Jefferson Hospital and prepared as described previously (23). HUVECs were cultured in M199 medium (Life Technologies, Inc., Rockville, MD), supplemented with 10% defined calf serum, 0.05% endothelial cell growth supplement (ECGS), 0.5% L-glutamine, 0.013% heparin sulfate, 0.5% penicillin/streptomycin, 0.05% gentamicin, and 0.5% fungizone. This medium also has a bicarbonate concentration of 26 mM and provided a pH_e 7.3 under 5% CO_2 and a pH_e 6.7 under 17% CO_2. HMVEC dermal adult cells were obtained from Clonetics (Walkersville, MD) and were maintained in Clonetics' medium.

Preparation of Cells for pH_i Experiments. For determination of pH_i, cells were plated on 35-mm microwell plastic dishes with glass coverslips glued to 1-cm diameter holes in the center of each dish (Mattek Corp., Ashland, MA). For melanoma cell experiments, coverslips were coated with a mixture of collagen I and RGD repeating peptides (Sigma) to provide a physiological substrate. RGD repeating peptides were used as a substitute for fibronectin. Collagen I and RGD peptides were both used at a final concentration of 50 μg/ml (24, 25). For experiments with HMT3522-T4/2 cells, coverslips were coated with a 1:3 dilution of Matrigel and serum-free medium as described previously (5). For experiments with NHEMs, coverslips were coated with fibronectin-like RGD fragments because fibronectin adhesion is thought to be critical to focal contact organization (26) and suppression of apoptosis in these cells (27). Cells were plated in the

microwell dishes at a density of 0.2–0.3 $\times$ 10^6 cells/ml in 2 ml of medium, 48–72 h before experiments were performed. Preliminary experiments (not shown) found that dye leakage over 1–2 h of an experiment was minimal (usually undetectable) if the cells were previously plated 48–72 h before the experiment and allowed to adjust to their substrate.

Dye Loading. Cells were incubated for 15 min with 9 μM C.SNARF-1-a.m. (28) or for 4 min with 5 μM BCECF-a.m. in medium containing 10% fetal bovine serum in a 37°C incubator under 5% CO_2 as described previously (5, 29). After a change of medium, the cells were further incubated for 20 min at 37°C, 5% CO_2 to complete the hydrolysis of the dye ester and to allow recovery from the dye loading. The plate was then mounted on the microscope stage for study at 37°C under flowing humidified air containing 5% CO_2. Experiments performed to assess steady state pH_i before and after acute acidification with and without inhibitors were performed using BCECF on a microscope geared to measure fluorescence spectrum shifts that occur in excitation spectra. The rapid measurements necessary for the ammonium chloride assays depicted in Fig. 4 were performed using C.SNARF, a dye that shifts its emission spectrum as a function of pH changes. The difference in choice of dye relates to the time necessary to acquire an excitation *versus* an emission spectrum, which is dictated by the speed for acquisition of the data. The acquisition time is a function of the type of light detector used to transduce the fluorescence signal and of the velocity and length of time that is necessary to drive an excitation *versus* an emission detector through a large number of wavelengths in the amount of time necessary to detect the changes in pH_i within the critical time frame in which they occur.

Inhibitors. Cariporide was freshly dissolved in deionized distilled H_2O at a concentration of 3 mM immediately before each experiment, then diluted to a final concentration of 60 μM in medium. DIDS was dissolved in DMSO at 0.2 M, and then diluted to 0.2 mM in α-MEM. The CNCn was dissolved in DMSO as a 500-mM stock and then was diluted in α-MEM medium to a final concentration of 10 mM in buffer or media, and then pH adjusted with NaOH to the experimental pH. This was then diluted to a final concentration of 10 mM on the microscope stage. The pH was stable for the duration of all of the experiments, which was confirmed with direct measurements of pH_e. DMSO and other vehicle controls were completely negative with respect to the effect on pH_i (data not shown). DBDS was made up as a 0.02 M stock solution and diluted to a final concentration of 0.3 mM. The results of dose-response experiments indicated which drug concentrations would give maximum pH_i effects (data not shown). For inhibitors that did not show activity, the concentrations used were similar to those that gave maximum responses in other cell lines tested in previous work (5).

Fluorescence Microscopy and Calibration. Cellular pH values were obtained from whole emission or excitation spectra that were measured on cells that remained attached to physiological substrate as described above. Samples on an inverted microscope (Nikon Diaphot; Nikon Inc.) were illuminated via fiber optic with a 75-W xenon light source equipped with a spectrofluorimeter that made 140 single wavelength measurements at 1-nm intervals, from 400 to 540 nm, to cover the entire excitation spectrum for BCECF. The excitation monochromator slit was 4 nm, and each reading had a 0.4 s/step integration time. The emission was detected using a filter cube containing a 510-nm dichroic mirror and a 520-nm emission interference filter (10-nm band width; Omega Optical, Brattleboro, VT) at 550 nm.

Another inverted microscope (Nikon Diaphot; Nikon Inc.) was used to collect emission spectra (for C.SNARF), as has been previously described (5, 28, 30, 31). Briefly, a fiber optic from a 75-W xenon lamp excited the dye at 510 nm., selected by monochromator. A filter cube transmitted the emission wavelengths above 540 nm to a spectrometer that projected the emission spectrum onto a CCD array. The resolution was slightly better than 1 nm/pixel of the CCD. All of the wavelengths of the emission spectrum were measured simultaneously, with light being collected for 5 s and the process repeated every 10 s. This system was used when rapid measurements were desired, as in the ammonium chloride assay (see Fig. 4).

In both cases, the use of the entire spectrum to determine pH_i is an improvement on the usual ratiometric dye technique, in part because 140 different measurements are made on each cell. This redundancy in the data results in a significant improvement in accuracy. The value of pH_i is obtained from a least-squares calculation that involves a form of averaging. Possibly, it is more important that background fluorescence (caused by phenol red and serum in the medium and light-scattering artifacts from cells) was measured on dye-free cells and then subtracted before the calculation was performed (31). In part because the microscope did not have a long working-distance objective, the fluorescence from the medium surrounding the cells was sufficiently small (and constant) that it could be subtracted from the data spectra. There was no detectable change in results when medium containing serum and phenol red was used, as compared with medium that was prepared without serum or the indicator (data not shown). In addition, there was no effect of matrix proteins on basis spectra or baselines.

All of the determinations were made on attached cells at 37°C in medium containing HCO_3^- under flowing 5% CO_2 to avoid underestimating Cl^-/HCO_3^- exchange (13). Assays determining NHE-1 activity and MCT activity were made under conditions optimal for maximum activity, *i.e.,* in the presence of serum (32), integrin engagement (33, 34), and during acute and/or chronic acidification (9, 16).

To make a single pH_i measurement, the spectrometer was stepped through all excitation wavelengths (in the case of BCECF), or else, the CCD on the emission spectrometer simultaneously acquired a signal for every wavelength in the emission spectrum (as for C.SNARF). A background spectrum was obtained from an identical plate of the same cells under identical conditions, except the cells were not loaded with fluorescent dye. The background spectrum was then subtracted from the data spectrum to obtain the signal that was attributable only to the dye itself. This spectrum was analyzed by a least-squares calculation to find the value of pH_i that was most consistent with the data.

Although the background spectrum was measured each day (in case cells should vary in light-scattering properties from one day to the next), the calibration of the instrument was performed only when a change was made in optical elements (adjustment of lamp, change of slit width, and so forth). A new calibration was also done whenever cells of a new type were being tested, but it was found that a change in cell type mainly affected the background spectrum but had little effect on instrument calibration. For example, it was expected that light scattering and other factors might be different enough to cause a problem when tissue fragments were analyzed. Accordingly, the system was recalibrated (see "Xenograft Microfragments" below) for xenograft fragments, but the calibration was found to be the same for cultured or tissue fragment DB-1 cells.

The calibration procedure for adherent cells containing either C.SNARF-1 or BCECF was essentially the same as that described by Grynkiewicz *et al.* (35) for fura-2, which is another "dual wavelength" ratiometric dye that is used to measure intracellular free calcium; however, fluorescence signals were measured at ~140 wavelengths rather than at only 2. In following the methods of Grynkiewicz *et al.* (35), cells were placed in a cytosol-like buffer and exposed to the ionophores nigericin and valinomycin to obtain a known pH_i (*i.e.,* equal to pH_e; Ref. 32). As in Grynkiewicz *et al.* (35), measuring the exact same visual field of cells at two different known values of pH (achieved by modifying buffer pH while on the microscope stage) allowed the computer program to calculate the fluorescence for the dye if it were in the fully protonated or the fully deprotonated state. This produced two "basis spectra," corresponding to the signal from intracellular dye at high pH (fully deprotonated) or low pH (fully protonated; Refs. 5, 30, 36). The computer program that analyzed each sample asked what mixture of these two basis spectra (36) would produce the least-squares best fit to the observed spectrum (31, 36, 37). The relative amounts of protonated- or deprotonated-basis spectra needed revealed the relative amounts of protonated and deprotonated dye in the cells. This information, and the Henderson Hasselbalch equation, together with the pK_a of the dye, provided the pH inside the cells.

The calibration of the system (a particular set of basis spectra) was tested by analyzing cells in which the pH_i was known because the cells were in cytosol-like buffer and exposed to nigericin and valinomycin (35). Measurements were made on several cell preparations over a period of several days and covering a range of pH_i values between 6.55 and 7.47. When the calculated pH_i values were compared with the expected values based on pH_e, the accuracy of the system was found to be within 0.01 pH units on some days and within 0.024 units, overall.

Protocol for Extended pH_i Time Courses. Dye-loaded cells in medium were mounted on the microscope stage, and steady-state values for pH_i were determined in 2 ml of media. The cells were then incubated with one or more inhibitors of pH regulation at pH_e 6.5, 6.7, or 7.3 for 1–2 h to measure the effects on pH_i in a solution. Results from such experiments were always compared with experiments in which pH_e was reduced in the absence of inhibitors of pH regulation. The inhibitors included: 0.2 mM DIDS, which preferentially inhibited the Na^+-dependent Cl^-/HCO_3^- exchanger (13, 14); 60 μM cariporide, which preferentially inhibited NHE-1 (12); and 10 mM CNCn, which preferentially inhibited H^+-linked monocarboxylate transporters, isoforms 1, 2, and 4 (see Table 1). These isoforms have various relative affinities for pyruvate and lactate as substrates (16, 18, 38, 39).

The experiments were performed in complete growth medium at 37°C, and cells remained adherent to the substrate to which they had attached during the previous 48–72 h. In each procedure, the first measurement was of steady-state pH_i in cells that were dye-loaded in growth medium at pH_e 6.7 or 7.3. The initial steady-state pH_i at pH_e 6.7 or 7.3 was measured several times on a field of 8–15 cells, and then the medium was replaced with medium containing inhibitors and/or a low pH_e. The pH_i was measured on a single field of cells three to five times every 15 min for 1 h. For long time-course experiments, new plates of cells that were freshly loaded with dye were provided every hour, and the experiment was repeated (as shown in Fig. 1*a*) using with one plate for 2 h, and no differences were observed between the approaches. Control experiments showed that the inhibitor solvents (vehicles) had no effect on pH_i.

Recovery from an Intracellular Proton Loading. NH_4Cl intracellular proton loading protocols were performed on substrate-attached cells in Hanks' buffer [HEPES, 4 mM $NaHCO_3^-$ (pH 7.3)] at 37°C as described previously (28, 40). The NH_4Cl procedure exposed cells to an intracellular acidification at a normal pH_e. The time course of the cell recovery allowed observation of proton transporters when they have been stimulated to a maximum degree. Rates of proton extrusion could then be compared between cell lines. During the recovery from cytosolic acidification, the rate of change, dpH_i/dt, was obtained from the slope of the graph of pH_i as a function of time. Groups of three data points were used to calculate each rate.

Recovery was monitored in the presence and absence of inhibitors to determine which transporters were most active under conditions of a large intracellular proton load. This differed from exposing cells to inhibitors in the presence of extracellular acidification, which only indirectly caused intracellular acidification.

To test the melanoma cell lines during an intracellular acidification, a particular field of 10–20 cells loaded with C.SNARF were placed on the microscope stage. They were then incubated with 50 mM NH_4Cl for 350 s. Three to five spectra were taken at 10-s intervals. Next, the buffer was changed to an NH_4Cl-free buffer, still at pH_e 7.3. The removal of NH_4Cl induced a rapid acidification as NH_3 exited the cell (40, 41). C.SNARF fluorescence was excited at 510 nm, and the recovery of cells from intracellular proton loading was monitored for 350 s or longer if recovery was incomplete. Every time point for a given experiment contained the average (±SD) of three to five measurements taken over a field. Each experiment was repeated at least twice, and the data from a representative experiment is presented as pH_i (±SD) *versus* time.

Experimental Approach/Statistics. Three to five consecutive spectra were collected every 15 min, and were

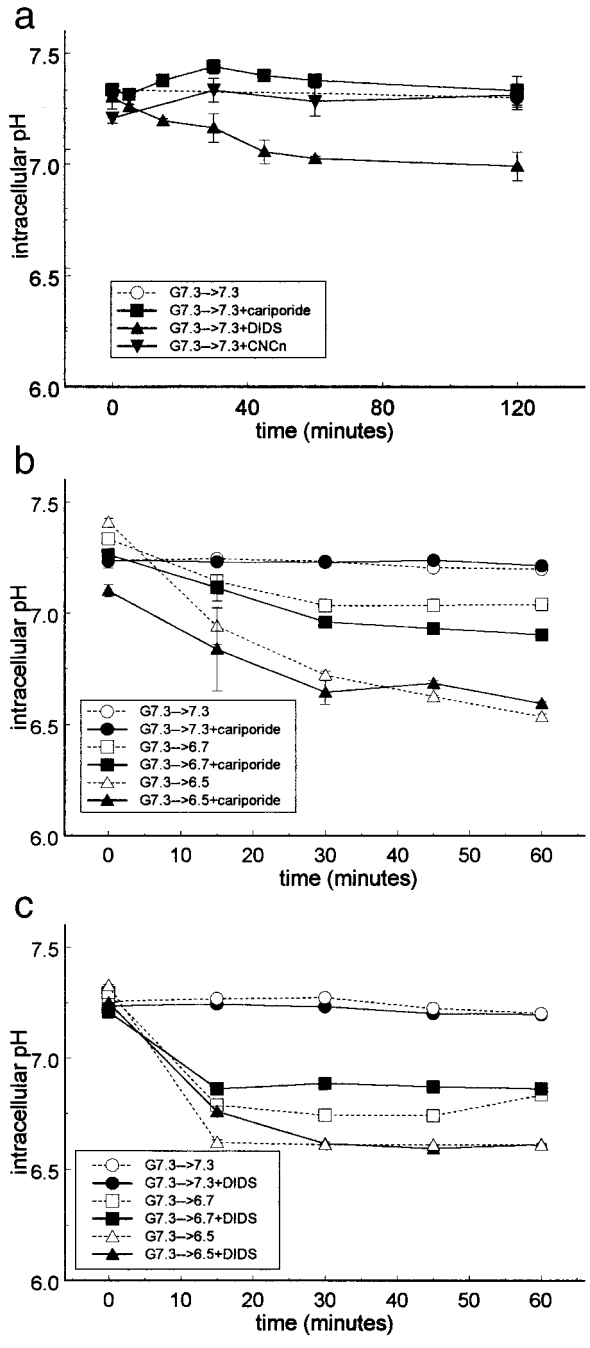

Fig. 1. *a*, the effect of single inhibitors on Sk-Mel-28 cells at their steady-state pH_e of 7.3. pH_i is shown as a function time for Sk-Mel-28 melanoma cells with no drug additions (○), or with 0.06 mM cariporide (■), with 0.2 mM DIDS (▲), or 10 mM CNCn (▼) added immediately after 0 time measurements were obtained. *b*, DB-1 cells at their growth pH_e without (○) and with (●) cariporide; acute extracellular acidification to pH_e 6.7 (□) and with cariporide (■); and acute extracellular acidification to pH_e 6.5 (△) and with cariporide (▲). Each graph is representative of two or more similar experiments performed on separate days. *Values* and *error bars*, means ± SDs. *c*, DB-1 cells at their growth pH_e without (○) and with (●) DIDS, acute extracellular acidification to pH_e 6.7 (□) and with DIDS (■), acute extracellular acidification to pH_e 6.5 (△) and with DIDS (▲). Each graph is representative of two or more similar experiments performed on separate days. *Values* and *error bars*, means ± SDs. Steady-state measurements were performed using cells containing BCECF using an excitation monochromator and a photon-counting detector (see also Figs. 2 and 3).

averaged to calculate a pH_i value for each 15-min interval with a SD. The error bars are not visible on the graphs when they are smaller than the symbols. Each experiment was repeated three or more times, and data from representative experiments are depicted in the Figures. All of the experiments were performed at least three times, but only one is shown in each case instead of averages because the initial pH_i varied slightly from plate to plate for all of the melanoma cell lines, although the magnitude of the pH_i changes in the case of various treatments did not. This was attributed to the clonal variation of the melanoma cells, because it was not observed in the nonmalignant and other malignant lines that were analyzed in the present study and in previously published work from this laboratory. This variation did not occur within one plate of cells when numerous fields were analyzed; rather, it was interplate variation.

Flow Cytometry. These experiments were performed using a CALTAG kit (Burlingame, CA) according to the manufacturer's instructions. Antibodies were polyclonal and raised in rabbits against the human antigens. NHE-1 antibody was obtained from Chemicon (Temecula, CA), and MCT-1 and MCT-2 antibody were obtained from David Golde (Memorial Sloan Kettering, New York, NY). Antibodies to MCT-1 and MCT-4 were also obtained from Andrew Halestrap (University of Bristol, Bristol, England). Briefly, cells were grown on fibronectin/collagen I substrate for 2 days, then released using Cell Stripper (Mediatech, Herndon, VA), a nonenzymatic agent, and rinsed in three changes of sterile, autoclaved, PBS buffer adjusted to the growth pH of the cells (6.7 or 7.3). Cells were counted and then resuspended at a concentration of 5×10^5 cells/250 μl in FACS medium [PBS, 0.1% sodium azide, 1% BSA (pH 7.0)]. All of the antibodies used in these experiments were directed toward the COOH-terminal ends of the transporters, located in the intracellular portion of the proteins, and, therefore, detergent permeabilization was necessary in each experiment to ensure primary antibody contact with the protein. Plates were centrifuged for 3 min at 1500 rpm, and the supernatant was removed. The 50 μl of reagent A (fixation medium) was added to each well and incubated for 15 min, followed by three washes in FACS medium. Cells were then incubated with primary antibody at room temperature for 45 min, washed, and then incubated with secondary antibody at room temperature for 45 min. Controls included cells incubated either with secondary antibody alone, or with no antibody, to measure nonspecific fluorescence and background fluorescence, respectively. Other nonmelanoma cell lines were also analyzed for comparison. Cells were monitored using a FACSCalibur flow cytometer (Becton Dickinson, Franklin Lakes, NJ) equipped with CellQuest software. Data are expressed as relative fluorescence.

RT-PCR. RNA was isolated from cells grown at normal and low pH after 2-days growth on a collagen I/fibronectin substrate. The purity and quantity of the RNA was assessed by measuring its absorbance at 260 nm and 280 nm and determining that the ratio of these absorbances was 1.5–2.0; a total protein-obtained harvest (20 million per harvest from each pair of T25 flasks) was 50 μg. Cells were detached from flasks using Cell Stripper (Mediatech, Herndon, VA) and then

were centrifuged in sterile PBS adjusted to the growth pH. RNA was prepared using RNAzol, as per instructions from Tel-Test Inc. (Friendswood, TX). The purity and quality of the RNA was determined by the appearance on a 1% agarose gel. The amount of RNA was quantitated using an AlphaImager 2200 equipped with the v5.5 program (Alpha Innotech Corp., San Leandro, CA), by comparison with a 100-bp nucleotide ladder (Promega, Madison, WI). cDNA was synthesized from total RNA using Superscript II RNAase H Reverse Transcriptase (Life Technologies, Inc., Rockville, MD) using random hexamer primers (Boehringer Mannheim, Indianapolis, IN) in the presence of 0.25 μl RNasin, (40units/μl; Promega, Madison, WI). Reverse transcription was carried out in an MJ Research, Inc. thermal cycler using a 60-min incubation at 42°C followed by 10 min at 50°C and 15 min at 70°C. The reaction was then cooled to 4°C and the random hexamers were removed using a QIAquick PCR purification kit (Qiagen Inc., Valencia, CA).

For the PCR reaction, 2.0 μl cDNA, 2.0 μl Aquanase (Tel Test Inc., Friendswood, TX), and 2.5 μl each of 10 μM forward and reverse primers were combined and heated for 2 min at 95°C in an MJ Research, Inc. thermal cycler and then cooled rapidly on ice. A master mix of 31.5 μl Aquanase, 5.0 μl of 10× PCR buffer, 2.0 μl 10 mM dNTPs (Amersham Pharmacia Biotech, Piscataway, NJ), and 2.5 μl Sigma Red Taq (Sigma) was added to the cDNA mixture. Cycle times were as follows: 2 min at 92°C; 35 cycles of 30 s at 92°C, 1 min at 50°C or 60°C; followed by 2 min at 72°C, 72°C, 5 min, 4°C, end), using transporter isoform-specific primers. The primers were obtained from Life Technologies, Inc. and were designed based on published sequences. An annealing temperature of 50°C was used for the MCT-1, MCT-4, and HUGAPDH208 primers, and 60°C for the NHE-1 and HUGAPDH325 primers. PCR samples were prepared using identical starting quantities of mRNA, using GAPDH message levels as an internal standard. PCR products were analyzed by size fractionation in a 1.4% agarose gel with a concentration of 0.5 μg/ml ethidium bromide (Life Technologies, Inc.).

Xenograft Microfragments. Fresh explants of human DB-1 tumor tissue (1–2 mm each) were excised from a SCID mouse on each of three occasions. SCID mice were anesthetized and tumor pH_e was measured with a 20-gauge needle combination microelectrode *in vivo* before sacrifice. The average pH_e of DB-1 mouse tumor xenografts were 6.68 ± 0.05. Samples of the tumor were excised and kept on ice in medium at pH 6.7 with 10% serum and 10 mM 2-[*N*-morpholino]-ethanesulfonic acid (to maintain pH 6.7 outside of an incubator with a 5% CO_2 atmosphere), dissected with a scalpel, and sieved through a metal mesh grid to divide them into small fragments between 10–20 cells in diameter. The microfragments were then affixed to microwell dishes using Cell-Tak tissue adhesive (Collaborative Biomedical Products, Bedford, MA) which had previously been layered onto microwell plates. Cells affixed to Cell-Tak were incubated for about 4 h at a pH_e that was the same as the measured pH_e *in situ* immediately before tumor excision (6.7). Other microfragments were incubated at 6.5 and 6.3. These were compared with microfragments incubated at the same pH_e in the presence of 10 mM CNCn.

Results

In steady state, pH_i of cells was first measured at time zero in complete medium at the growth pH_e of the cells. In control runs, the cells and medium were monitored with no further perturbation. The effects of inhibitors on pH_i were then tested by incubating cells with inhibitors, either at pH_e 7.3 or during extracellular acidification to 6.7 or 6.5 after the initial steady-state pH_i was taken at time zero. Whenever the pH_i decrease in the presence of inhibitor was significantly greater than that caused by acute acidification alone, it indicated that a particular transporter was active in that cell type.

The Effect of Ion Transport Inhibitors at pH_e 7.3. After a steady-state measurement was made, cells were exposed to 60 μM cariporide, 0.2 mM DIDS, or 10 mM CNCn, and pH_i was monitored for an additional 1–2 h. All three of the cell lines were tested with all three of the inhibitors at pH_e 7.3. Under these conditions, an effect on pH_i was observed in only one instance. Sk-Mel-28 cells in the presence of DIDS exhibited a decrease in pH_i of about 0.2 unit within 1 h. No detectable change in pH_i occurred in the presence of either cariporide or CNCn for these cells (Fig. 1*a*). Similarly, no detectable effects were seen after administration of any of the inhibitors in DB-1 and DB-8 melanoma cells at pH_e 7.3 (data not shown). These results were not unexpected, because the Cl^-/HCO_3^- exchanger had previously been reported in other cells to be the only transporter active at pH_e 7.3 (13).

The Effect of Ion Transport Inhibitors When Combined with Acute Acidification to 6.7 or 6.5. Following the experience in other cell types in which NHE-1 activity was the cell's prime defense against extracellular acidification (13), this was what was tested first in the melanoma cells. In Fig. 1*b*, *dashed lines* (controls, with *open symbols*) show the effect of various pH_e on pH_i in DB-1 cells in the absence of any inhibitor. The *solid lines* with *filled symbols* show the additional effect of cariporide at each pH_e tested. It was striking that cariporide did not lower pH_i under conditions that were previously found to be optimal for inhibiting NHE-1 activity in other cell types (12), which included acidification to pH_e 6.7 or 6.5. Similar results were obtained in experiments on Sk-Mel-28 and DB-8 melanoma cells (data not shown).

Fig. 1*c* depicts an evaluation of a Cl^-/HCO_3^- exchange inhibitor during acidification on pH_i. The *dashed lines* with *open symbols* show the effect of acute acidification to pH_e 6.7 and 6.5 alone on DB-1 cells (without inhibitor). The *solid lines* with *filled symbols* show that there was no effect of DIDS at pH_e 7.3, 6.7, or 6.5. Similar results were obtained using DB-8 cells (data not shown).

Fig. 2*a* depicts an evaluation of MCT activity using 10 mM CNCn in DB-1 melanoma cells with different degrees of extracellular acidification. As previously stated, there was a negligible effect of CNCn at pH_e 7.3 (*open versus filled circles*). Acidification alone, from pH_e 7.3 to 6.7, reduced pH_i by ~0.30 units (*open squares*) from 7.23 ± 0.03 to 6.93 ± 0.01. With the addition of CNCn, the pH_i further decreased to 6.70 ± 0.02; a total acidification of ~0.53 units (*filled squares*). Acidification to pH_e 6.5 lowered pH_i to 6.66 ± 0.01, a change of ~0.57 units (*open triangles*), and the inclusion of CNCn lowered it further, to 6.23 ± 0.03 a total of ~1.00 pH

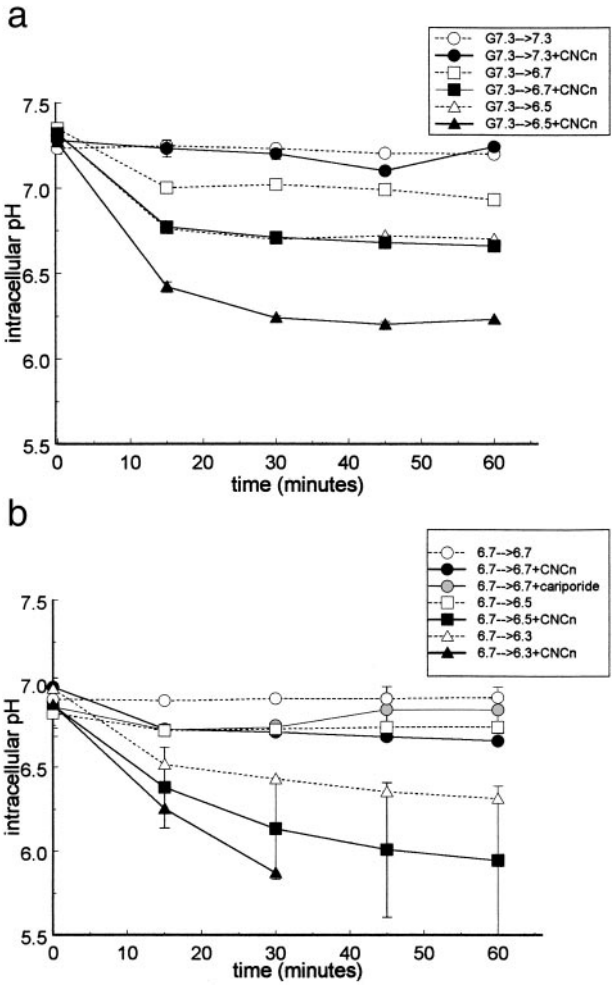

Fig. 2. *a*, the effect of acute acidification to pH_e 6.7 or 6.5 with CNCn on DB-1 melanoma cells. DB-1 cells at their growth pH_e without (○) and with (●) CNCn, acute extracellular acidification to pH_e 6.7 (□) and with CNCn (■), and acute extracellular acidification to pH_e 6.5 (△) and with CNCn (▲). Each graph is representative of two or more similar experiments performed on separate days. *Values* and *error bars*, means ± SDs. *b*, the effect of acute acidification to pH_e 6.5 or 6.3 with CNCn on DB-1 melanoma cells adapted to growth at pH_e 6.7 (26 mM HCO_3^-; 17% CO_2). DB-1 cells at their growth pH_e (6.7) without (○) and with (●) CNCn, and with cariporide (*gray filled circles*), acute extracellular acidification to pH_e 6.5 (□) and with CNCn (■), and acute extracellular acidification to pH_e 6.3 (△) and with CNCn (▲). Each graph is representative of two or more similar experiments performed on separate occasions. *Values* and *error bars*, means ± SDs.

units (*filled triangles*). All of these changes occurred within 30 min and were stable for 1 h. These results consistently indicate a greater level of dependence on MCT activity with increasing extracellular acidification, presumably because of increased rates of passive leakage of protons into the cells and possibly greater production of protons and lactate inside (42).

For a comparison, experiments were performed with two different primary cultures of NHEM. The initial pH values were 7.20 ± 0.03 and 7.06 ± 0.01. The final pH_i after 1 h of acidification to pH_e 6.5 was 6.60 ± 0.01 and 6.81 ± 0.01, respectively (data not shown). Acidification with cariporide at pH_e 6.5 caused pH_i to decrease to 6.54 ± 0.01 and 6.67 ± 0.01, respectively (data not shown). These effects represented changes in pH_i attributable to the drug exposure of 0.06 and 0.14, respectively. The finding with cariporide was consistent with a study elsewhere in which NHEM also exhibited NHE-1 activity (11).

Inhibitors of MCT-1 Acting on DB-1 Cells Adapted to Growth at Low pH_e. The steady-state pH_i value for DB-1 melanoma cells grown at pH_e 6.7 and measured at pH_e 6.7 was ~6.90. Similar values were seen with the other two melanoma cell lines. These were detectably lower than the steady-state values for cells that were grown at pH_e 7.3 and that were measured also at their growth pH_e.

Fig. 2*b* shows that CNCn had a noticeable effect on the cells grown at pH_e 6.7, reducing pH_i by about 0.25 unit when they were tested at pH_e 6.7 (*filled black circles*). This is comparable with the 0.30-pH-unit effect that CNCn had on cells grown at pH_e 7.3 when they, too, were tested at pH_e 6.7 (Fig. 2*a*).

When the low-pH-adapted cells were acidified to pH_e 6.5 (Fig. 2*b*, *open squares*), the effect that could be attributed to CNCn (*filled squares*) was more than an additional 0.5 unit. In fact, the pH_i measured <6.0 within 1 h of lowering the pH_e. Actual data values below a pH of 6.0 are not reported because limitations of the BCECF dye itself preclude making measurements with precision below that value. Nevertheless, it is clear that the low-pH-adapted cells appeared to be more dependent on MCT-mediated proton removal than did the cells grown at pH_e 7.3. When the latter were tested at pH_e 6.5, the effect of CNCn was to reduce pH_i by 0.43 unit, which only brought it down to 6.23 (Fig. 2*a*). By way of comparison, cariporide did not lower pH_i in the low-pH-adapted DB-1 cells when it was combined with acidification to 6.5 (Fig. 2*b*, *filled gray circles*) which is indicative of low NHE-1 activity.

When low-pH-adapted cells were acidified to pH_e 6.3 (Fig. 2*b*, *open triangles*), CNCn (*closed triangles*) caused a pH reduction to below pH_i 6.0 within 30 min. Although pH values cannot be stated with precision in this range, it was clear that, for an additional 60 min, pH_i remained below 6.0, and the cells remained intact in the sense that the dye was well retained.

An additional MCT inhibitor confirmed the changes in pH_i in all three of the cells lines tested. This was DBDS, which is primarily an MCT-1 inhibitor and which has the advantage of exclusion from the cell interior because of highly charged sulfonic moieties that cause a lack of ability to enter into cells and negligible effects on mitochondrial monocarboxylic acid transport as a result (43). In Fig. 3, the effects of DBDS on DB-1 cells grown at pH_e 7.3 and monitored at pH_e 7.3, 6.7, or 6.5 are shown. The results are similar to those obtained using CNCn. DBDS did not affect pH_i at pH_e 7.3 (*open* and *filled circles*) but did cause pH_i to decrease when combined with acidification to pH_e 6.7 (*open* and *filled squares*), and even more so with acidification to pH_e 6.5 (*open* and *filled triangles*).

Recovery from Intracellular Acidification in Melanoma Cells, Breast Cells, and Keratinocytes and Assessment of Buffering Capacity. Fig. 4*a* shows the patterns of recovery of pH_i that have typically been observed in other cell

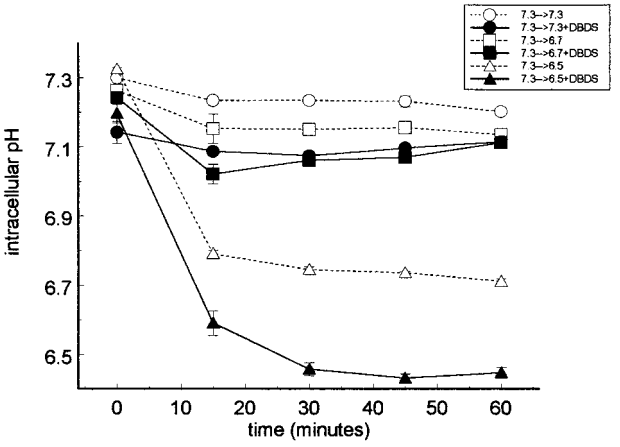

Fig. 3. Effects of DBDS and/or acute extracellular acidification on DB-1 cells grown at pH_e 7.3. DB-1 cells at their growth pH_e (7.3) without (○) and with (●) DBDS, and acute extracellular acidification to pH_e 6.7 (□) and with DBDS (■), and acute extracellular acidification to pH_e 6.5 (△) and with DBDS (▲). The graph is representative of two or more similar experiments performed on separate occasions. *Values* and *error bars*, means ± SDs.

types (HMT3522-T4/2 malignant breast cells in this case). The recovery rate (expressed as dpH_i/dt, the slope of the graph shown) reached 0.25 ± 0.64 (n = 4) pH unit/min (*open circles*). These cells fully returned to their initial steady-state pH_i within 350 s after the removal of ammonium chloride (ammonium chloride challenge itself is not shown in Fig. 4).

When NHE-1 was inhibited by cariporide, the recovery rate was reduced to 0.06 ± 0.02 (n = 4) pH unit/min (Fig. 4, *inverted filled triangles*), and cells did not return to their initial pH_i. Recovery was not affected by DIDS (*filled triangles*) or CNCn (*filled squares*), which indicated that the Cl^-/HCO_3^- exchanger and MCTs did not figure prominently in this recovery. The nonmalignant counterpart of HMT3522-T4/2, called HMT3522-S1 (44), exhibited identical recovery profile and responses to inhibitors (data not shown). In a similar experiment, recovery from intracellular acidification was measured in keratinocytes (HaCaT cells) with inhibitors present or absent during the recovery (Fig. 4*b*). The rate of recovery was 0.11 ± 0.03 pH unit/min (*open circles*), which was ~100% inhibited by 60 μM cariporide (*filled inverted triangles*), to a rate of 0.007 ± 0.002 pH unit/min (n = 4). Again, recovery was not affected by DIDS (*filled triangles*) or CNCn (*filled squares*).

In contrast to all three of these cell lines, Sk-Mel-28 cells, grown at pH_e 7.3, depicted in Fig. 4*c*, had a recovery during resuspension that was slow and incomplete, at an average rate of 0.06 ± 0.01 pH unit/min (n = 4). DB-1 and DB-8 cells had similar profiles (data not shown). These rates are representative of at least four experiments each. The *filled symbols* show inhibitor effects, which were only barely discernable with CNCn and not at all discernable with DIDS and cariporide.

For cells grown at pH_e 7.3, the final values of pH_i that were reached for both of the melanoma cells lines were less than 6.8, although both cell lines had original steady-state pH_i values between 7.20 and 7.30. Experiments were also performed monitoring recovery for an additional 350 s or incubating cells after treatment and measuring pH_i after 24 h. No further recovery of pH_i was observed (data not shown). These data are similar to results obtained by two other in-

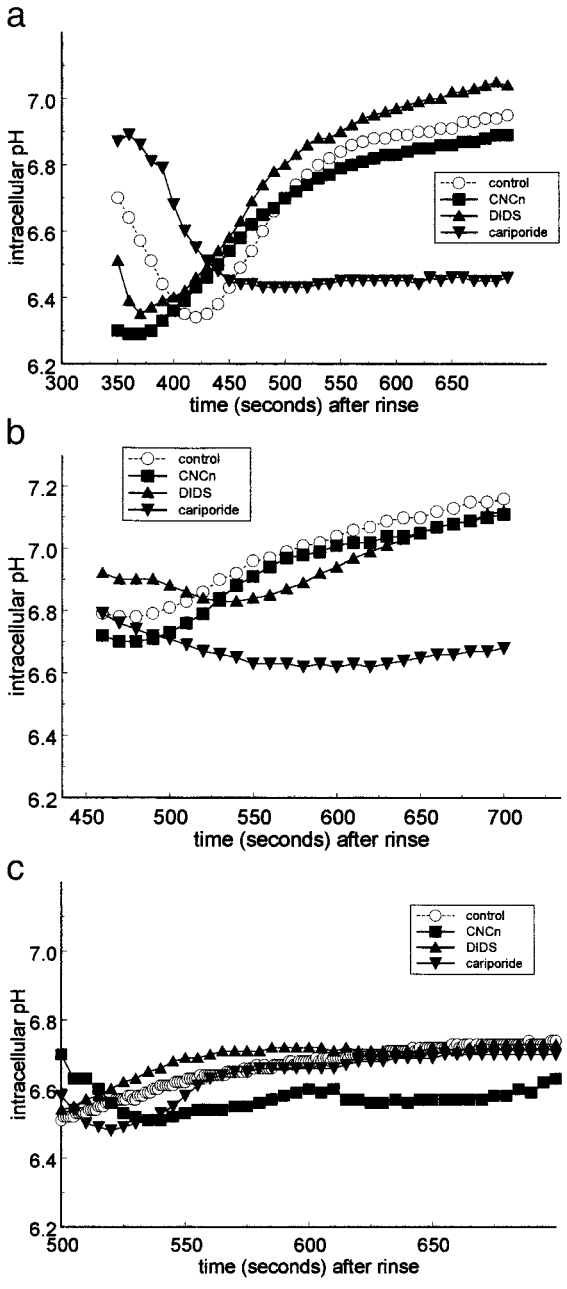

Fig. 4. *a*, recovery from intracellular acidification induced by incubation with NH_4Cl followed by a rinse at pH_e 7.3 in HMT3522-T4/2 cells. Control (○), with cariporide (▼), with CNCn (■), and with DIDS (▲). Rapid whole spectrum measurements were made on intracellular C.SNARF using an emission spectrometer and a CCD camera in *a*–*c*. *b*, recovery from intracellular acidification induced by incubation with NH_4Cl followed by a rinse at pH_e 7.3, in HaCaT cells (keratinocytes). Control (○), with cariporide (▼), with CNCn (■), and with DIDS (▲). *c*, recovery from intracellular acidification induced by incubation with NH_4Cl followed by a rinse at pH_e 7.3 in Sk-Mel-28 cells grown at pH_e 6.7C. Control (○), with cariporide (▼), with CNCn (■), and with DIDS (▲).

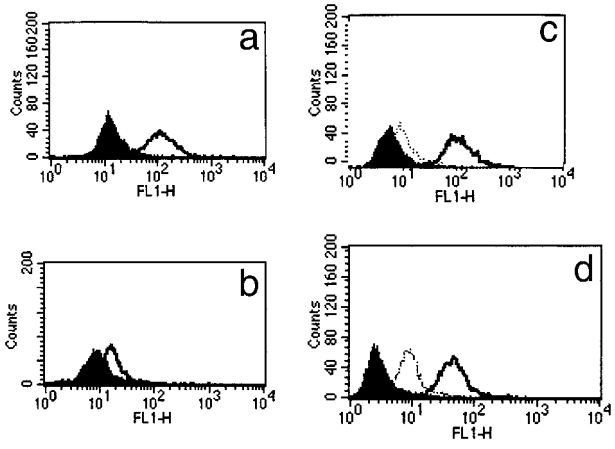

Fig. 5. Flow cytometry on MCT-1, MCT-4, and NHE-1 showing an experiment with DB-1 cells. *a*, MCT-1 expression shown in DB-1 cells grown at pH_e 7.3 (*filled peak*) overlaid with DB-1 cells grown at pH_e 6.7 (*open peak*), both stained with primary (*anti-MCT-1*) and secondary antibodies. There is significant up-regulation of the MCT-1 at low pH. *b*, MCT-4 expression shown in DB-1 cells grown at pH_e 7.3 (*filled peak*) overlaid with DB-1 cells grown at pH_e 6.7 (*open peak*), both stained with primary (*anti-MCT-4*) and secondary antibodies. There is slight up-regulation of the MCT-4 at low pH. *c*, background (*solid peak*), MCT-1 expression (*open peak*, *solid line*), and MCT-4 expression (*open peak*, *dashed line*) in HaCaT cells grown at pH_e 7.3. *d*, background (*solid peak*), MCT-1 expression (*open peak*, *solid line*), and MCT-4 expression (*open peak*, *dashed line*) in HUVECs grown at pH_e 7.3.

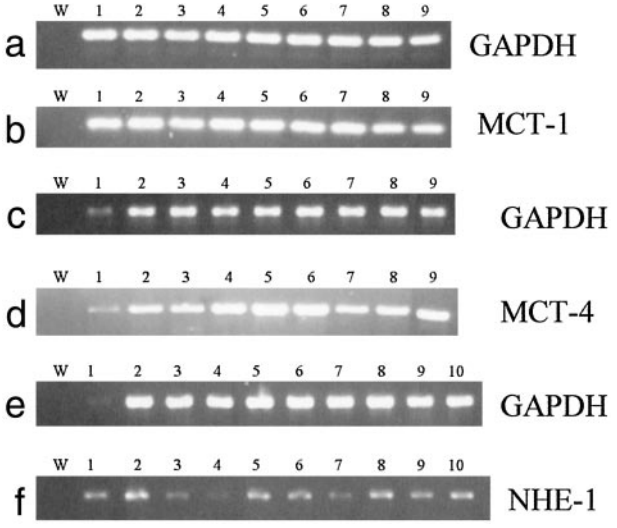

Fig. 6. RT-PCR showing mRNA levels of the transporters. *Lane w* of each agarose gel, a water control. *a* and *b*, GAPDH and MCT-1 expression in cells: *Lane 1*, HaCaT cells; *Lane 2*, DB-1 cells (pH_e 6.7); *Lane 3*, DB-1 cells (pH_e 7.3); *Lane 4*, DB-8 cells (pH_e 6.7); *Lane 5*, DB-8 cells (pH_e 7.3); *Lane 6*, Sk-Mel-28 cells (pH_e 6.7); *Lane 7*, Sk-Mel-28 cells (pH_e 7.3); *Lane 8*, HMVECs (pH_e 6.7); *Lane 9*, HMVECs (pH_e 7.3). *c* and *d*, GAPDH and MCT-4 expression in cells: *Lane 1*, HaCaT; *Lane 2*, DB-1 cells (pH_e 6.7); *Lane 3*, DB-1 cells (pH_e 7.3); *Lane 4*, DB-8 cells (pH_e 6.7); *Lane 5*, DB-8 cells (pH_e 7.3); *Lane 6*, Sk-Mel-28 cells (pH_e 6.7); *Lane 7*, Sk-Mel-28 cells (pH_e 7.3); *Lane 8*, HMVECs (pH_e 6.7); *Lane 9*, HMVECs (pH_e 7.3). *e* and *f*, GAPDH and NHE-1 expression in cells: *Lane 1*, PS120 cells; *Lane 2*, HaCaT cells; *Lane 3*, DB-1 cells (pH_e 6.7); *Lane 4*, DB-1 cells (pH_e 7.3); *Lane 5*, DB-8 cells (pH_e 6.7); *Lane 6*, DB-8 cells (pH_e 7.3); *Lane 7*, Sk-Mel-28 cells (pH_e 6.7); *Lane 8*, Sk-Mel-28 cells (pH_e 7.3); *Lane 9*, HMVECs (pH_e 6.7); *Lane 10*, HMVECs (pH_e 7.3).

vestigators using a total of eight other melanoma cell lines (11, 45).

Flow Cytometry Using Antibodies to MCT-1, MCT-4, NHE-1. Fig. 5, *a* and *b*, show that MCT-1 and MCT-4 proteins were present in DB-1 cells grown at pH_e 7.3 (*filled peaks*), and may be enriched in melanoma cells grown at pH_e 6.7 (Fig. 5, *c* and *d*, *open peaks*). In this experiment, the levels of MCT-4 were elevated ~2- to 3-fold, and MCT-1 was elevated ~10-fold in DB-1 cells grown at pH_e 6.7 as compared with those grown at pH_e 7.3. In Sk-Mel-28 cells, the elevations of bound antibody were less reproducible. DB-8 cells had high levels of both MCT-1 and MCT-4 even in cells grown at 7.3, and showed correspondingly less enhancement under low pH conditions. All three of the melanoma cell lines also had detectable NHE-1 protein, shown elsewhere in five other melanoma cell lines (11). The present study showed that NHE-1 levels were unaffected by growth at low pH in all three of the cell lines (data not shown). The results are consistent with the possibility that up-regulation of MCTs may have been an important mechanism by which these three melanoma cell lines maintained pH_i while being grown at a low pH_e. MCT-1 levels in melanoma cells grown at pH_e 7.3 were similar to those observed in HaCaT and HUVEC (Fig. 5, *c* and *d*, *open peak*, *solid line*), but MCT-4 levels were higher in melanoma cells (*open peak*, *dashed line*). The flow cytometric data were consistent with the inhibitor data, which indicated that MCTs are up-regulated, with changes in expression levels being clearly reproducible in DB-1 cells and slightly less consistent in Sk-Mel-28 cells. In DB-8 cells the levels of MCT were high when cells were grown at either pH_e.

RT-PCR. RT-PCR was performed on three melanoma cell lines (DB-1, DB-8, and Sk-Mel-28), as well as on HaCaT cells, HMVECs, and PS120 cells. PS120 cells are transfectants that overexpress NHE-1. Results (Fig. 6) showed no up-regulation as a function of low pH_e at the transcriptional level. Cells grown at normal pH did not differ in message levels from the nonmalignant cell lines of different origins with which they were compared. These data imply that up-regulation of MCTS and NHE-1 occurred at the level of translation, or posttranscriptional modification.

Effects of an MCT-1 Inhibitor on Fresh Xenograft Explants from DB-1 Tumors Maintained in SCID Mice. The sensitivity of DB-1 cells to inhibition by CNCn was further tested in fresh explants from xenografts grown in SCID mice. Before tissue was explanted, pH_e was measured *in vivo* using a microelectrode as described in "Materials and Methods," and the value obtained was consistently 6.68 ± 0.05. Fresh explants were then incubated for 20 h at pH_e 6.7, 6.5, or 6.3 in the presence and absence of CNCn. The results shown in Table 2 indicate that pH_i in the tissue fragments (which were without actively perfused medium) was lower than in isolated cells that were bathed in the same medium when grown in culture. The pH_i was also less sensitive to the pH_e in the medium outside the fragment than was the case for cells on a tissue culture plate. However, the cells were alive, as indicated by their uptake and retention of BCECF dye, and they were sensitive to CNCn. In particular, at pH_e

Table 2 The effect on pH_i in DB-1 xenograft microfragments of chronic and acute acidification in the presence and absence of CNCn

pH_i	pH_i without CNCn	pH_i with CNCn
6.7	6.34 ± 0.001 (4)[a]	6.05 ± 0.002 (4)
6.5	6.43 ± 0.004 (4)	6.07 ± 0.004 (4)
6.3	6.26 ± 0.003 (4)	<6.00 ± 0.002 (4)

[a] 4 samples of tissues.

6.3, CNCn caused pH_i to decrease to values below pH_i 6.0. This decrease was sustained for 1 h without dye leakage. The results show that CNCn could significantly compromise pH_i in a xenograft, in which cells *in situ* retain the cell-cell contacts.

Discussion

Three families of transporters that are found in the plasma membrane are designed to maintain pH_i in the viable range. Although many cells are known to rely on all three families, the melanoma cells in this study were uniquely dependent on the MCT family. MCTs, most commonly known in the literature as "lactate-proton *sym*porters," remove both lactate and H^+ (in the same direction). The MCT could be passive in that no other reaction is coupled to serve as a source of energy (*e.g.,* no hydrolysis of ATP or transport of Na^+). No other ion gradients are involved besides the gradients of lactate anions and the H^+ themselves. In a tumor with an acidic milieu, energy stored in a lactate gradient could be used to drive H^+ transport against its transmembrane gradient, as originally described by Warburg (46). That the MCT would be the predominant proton-removal mechanism for any cells, and especially for cells in an extracellular medium of reduced pH, was unexpected, given that the combined lactate and H^+ gradients provide the only free energy that is available for the joint transport.

Changes in pH_i, as well as the regulation of pH_i, have been studied in a number of tumor types. Activities of transporters that affect pH_i have been connected to the cell cycle (32, 47–49), cell migration (50), and drug resistance (51), and to potential for metastasis (45, 52). In many solid tumors in which pH_e is lower than normal, individual cell survival requires that cells there develop mechanisms for the control of pH_i that can remain active despite the increase in the free energy that is required to remove metabolic protons from the interior of the cell. Because tumor cells are often found at a low pH_e, even one that would normally compromise the viability of cells, it is of interest to understand the mechanisms by which these cells cope with the challenge of increased extracellular proton concentration. Selective inhibition of such mechanisms can also be explored as a way to increase stress on tumor cells and aid, for example, in chemotherapy or hyperthermia treatment.

Melanoma is a notoriously heterogeneous disease in terms of phenotypic and genotypic characteristics (53) and of response to therapy (54). It is, therefore, noteworthy that the three melanoma cell lines examined were strikingly similar with respect to pH_i regulation. The data are suggestive that Sk-Mel-28 cells had two of the three major pH-regulating transporters. At a growth pH_e of 7.3, they primarily used the Cl^-/HCO_3^- exchanger. The MCTs were induced by extracellular acidification, but there was little NHE-1 activity even at low pH_e. DB-1 and DB-8 cells also exhibited little NHE-1 activity and significant MCT activity, and these also lacked measurable Cl^-/HCO_3^- exchange.

In an acidified medium, H^+ removal via the MCT would require an increase in intracellular lactate and H^+ levels to force flow in the outward direction. It is not known why melanoma cells rely on this mechanism rather than on NHE-1, which could draw on the energy of the sodium gradient and would be expected *a priori* to be more effective at transporting protons against a greater proton gradient in acidified environments. Such a dependence on the MCT has not been observed in any of the normal cells or other tumor cell types tested in this laboratory, nor has it been reported elsewhere. Interestingly, it also contrasts with keratinocytes (which typically surround melanomas) and melanocytes (the cells of origin). Both of these showed typical NHE-1 activity.

In the intracellular acidification challenge assay, melanoma cells did not recover rapidly or fully, even in control experiments without inhibitors present. Cells are usually thought to use the NHE-1 to recover from intracellular acidification, so their poor recovery during this assay is additional evidence that NHE-1 activity is low in these melanoma cell lines. Similar results from assays testing NHE-1 function have been reported in a total of nine other melanoma cell lines by two different investigators (11, 45). Our data in the present study, for three other melanoma cell lines and two other melanocyte lines, are consistent with those data.

Many previous studies using CNCn or quercetin have focused on lactate transport (16, 38, 39, 55, 56), but none have directly measured concomitant effects on pH_i. *MCT-1* gene expression has been studied in some tumors (57) exclusive of melanoma, and MCT-4 levels have not been measured previously in any tumors. This is, therefore, the first demonstration that the MCTs appear to be critical for maintaining pH_i in the viable range in any cell type. It was also necessary to study tumor cells under low pH_e conditions for the MCT activity to be manifest. This work indicates that inhibitors of MCTs could be useful adjuncts to melanoma therapy, with particularly high activity in areas of tumors in which pH_e is low, giving them a built-in selectivity for the tumor bed. It is because of their low NHE-1 activity that inhibitors of MCTs would be expected to be particularly effective in melanoma as opposed to other tumor types.

One caveat with respect to the experiments using CNCn (18) is that CNCn may also act on mitochondria to inhibit pyruvate entry via a MCT variant, which could cause increased lactate and H^+ production. This secondary effect could contribute to the decrease in pH_i observed in experiments with CNCn because the inhibited MCTs might be trying to keep up with the increased proton production. Two lines of evidence suggest that metabolic shifts involving increased lactate and proton production are not the principal reason for the observed decreases in pH_i. First, measurements of lactate production when the extracellular milieu was acidified found it to be reduced, rather than increased (42). Second, when the inhibitor DBDS was used instead of

CNCn, it produced the same results. The sulfonate side chains of DBDS have been reported to preclude its entry into cells, with the result that it acts only on the plasma membrane MCT (43). Other considerations that pertain *in vivo* are the level of hypoxia and blood flow levels, which are not addressed in the present study.

In conclusion, the data presented here indicate that MCTs are the major functional transporters in melanoma cells. Inhibitors of MCTs have a great potential to selectively compromise melanoma cell viability and to improve the effectiveness of chemotherapeutic drugs that are more effective at low pH_i/pH_e, such as alkylating agents and platinum-containing compounds, while sparing normal and surrounding cells that are not in regions of low pH_e.

Acknowledgments

We thank David Golde (Memorial Sloan Kettering, New York, NY) and Andrew Halestrap (University of Bristol, Bristol, United Kingdom) for generous provision of antibodies to the isoforms of the MCT and for helpful discussions. We thank Derrick S. Grant (Cardeza Foundation, Department of Medicine, Thomas Jefferson University, Philadelphia, PA) for generous provision of HUVECs. We also would like to thank Crystal M. Fleming, Kiana Fulcher, Amos Ladouceur, Shari Lee, Marea Pollard, and Angela R. Page for expert technical assistance.

References

1. Yamagata, M., and Tannock, I. F. The chronic administration of drugs that inhibit the regulation of intracellular pH: *in vitro* and anti-tumour effects. Br. J. Cancer, *73:* 1328–1334, 1996.

2. Lyons, J., Ross, B., and Song, C. W. Enhancement of hyperthermia effect *in vivo* by amiloride and DIDS. Int. J. Radiat. Oncol. Biol. Phys., *25:* 95–103, 1993.

3. Leeper, D. B., Engin, K., Wang, J. H., Cater, J. R., and Li, D. J. Human tumor extracellular pH as a function of blood glucose concentration. Int. J. Radiat. Oncol. Biol. Phys., *28:* 935–943, 1994.

4. Leeper, D. B., Engin, K., Wang, G. J., and Li, D. J. Effect of i.v. glucose *versus* combined i.v. plus oral glucose on human tumour extracellular pH for potential sensitization to thermoradiotherapy. Int. J. Hyperthermia, *14:* 257–269, 1998.

5. Wahl, M. L., Pooler, P. M., Briand, P., Leeper, D. B., and Owen, C. S. Intracellular pH regulation in a nonmalignant and a derived malignant human breast cell line. J. Cell. Physiol., *183:* 373–380, 2000.

6. Grinstein, S. Activation of sodium-hydrogen exchange by mitogens. *In:* S. Grinstein, J. D. Smith, S. H. Benedict, and E. W. Gelfand (eds.), Current Topics in Membranes and Transport, Vol. 34, pp. 331–343. New York: Academic Press, Inc., 1989.

7. Sardet, C., Franchi, A., and Pouyssegur, J. Molecular cloning, primary structure and expression of the human growth factor-activatable Na^+/H^+ antiporter. Cell, *56:* 271–280, 1989.

8. Tse, C-M., Levine, S. A., Yun, C. H. C., Nath, S., Pouyssegur, J., and Donowitz, M. Molecular properties, kinetics and regulation of mammalian Na^+/H^+ exchangers. Cell Physiol. Biochem., *4:* 282–300, 1994.

9. Orlowski, J., and Grinstein, S. Na^+/H^+ exchangers of mammalian cells. J. Biol. Chem., *272:* 22373–22376, 1997.

10. Fliegel, L., Murtazina, R., Dibrov, P., Harris, C., Moor, A., and Fernandez-Rachubinski, F. A. Regulation and characterization of the Na^+/H^+ exchanger. Biochem. Cell Biol., *76:* 735–741, 1998.

11. Sarangarajan, R., Shumaker, H., Soleimani, M., Poole, C. L., and Boissy, R. E. Molecular and functional characterization of sodium-hydrogen exchanger in skin as well as cultured keratinocytes and melanocytes. Biochim. Biophys. Acta, *1511:* 181–192, 2001.

12. Scholz, W., Albus, U., Counillon, L., Gogelein, H., Lang, H. J., Linz, W., Weichert, A., and Scholkens, B. A. Protective effects of HOE642, a selective sodium-hydrogen exchange subtype inhibitor, on cardiac ischaemia and reperfusion. Cardiovasc. Res., *29:* 260–268, 1995.

13. Reinertsen, K., Tonnessen, T., Jacobsen, J., Sandvig, K., and Olsnes, S. Role of chloride/bicarbonate antiport in the control of cytosolic pH. J. Biol. Chem., *263:* 1117–1125, 1988.

14. Cassel, D., Scharf, O., Rotman, M., Cragoe, E., and Katz, M. Characterization of Na^+-linked and Na^+-independent Cl^-/HCO_3^- exchange systems in Chinese hamster lung fibroblasts. J. Biol. Chem., *263:* 6122–6127, 1988.

15. Juel, C., and Halestrap, A. P. Lactate transport in skeletal muscle-role and regulation of the monocarboxylate transporter. J. Physiol. (Lond.)., *517:* 633–642, 1999.

16. Halestrap, A. P., and Price, N. T. The proton-linked monocarboxylate transporter (MCT) family: structure, function, and regulation. Biochem. J., *343:* 281–299, 1999.

17. Manning Fox, J. E., Meredith, D., and Halestrap, A. P. Characterisation of human monocarboxylate transporter 4 substantiates its role in lactic acid efflux from skeletal muscle. J. Physiol. (Lond.), *529:* 285–293, 2000.

18. Halestrap, A. P., and Denton, R. M. Specific inhibition of pyruvate transport in rat liver mitochondria and human erythrocytes by α-cyano-4-hydroxycinnamate. Biochem. J., *138:* 313–316, 1974.

19. Clarke, P. D., Clift, D. L., Dooldeniya, M., Burnett, C. A., and N. A., C. Effects of α-cyano-4-hydroxycinnamic acid on fatigue and recovery of isolated mouse muscle. J. Muscle Res. Cell Motil., *16:* 611–617, 1995.

20. McNeill, H., and Jensen, P. J. A high-affinity receptor for urokinase plasminogen activator on human keratinocytes: characterization and potential modulation during migration. Cell Regul., *1:* 843–852, 1990.

21. Graeven, U., Fielder, W., Karpinski, S., Ergun, S., Kilie, N., Rodeck, U., Schmiegel, W., and Hossfeld, D. K. Melanoma-associated expression of vascular endothelial growth factor and its receptors FLT-1 and KDR. Cancer Res., *11:* 621–629, 2001.

22. Vexler, Z. S., Symons, M., and Barber, D. L. Activation of Na+-H+ exchange is necessary for rhoA-induced stress fiber formation. J. Biol. Chem., *271:* 22281–22284, 1996.

23. Grant, D. S., Kinsella, J. L., Kibbey, M. C., LaFlamme, S., Burbelo, P. D., Goldstein, A. L., and Kleinman, H. K. Matrigel induces *thymosin β4* gene in differentiating endothelial cells. J. Cell Sci., *108:* 3685–3694, 1995.

24. Petitclerc, E., Stromblad, S., von Schalscha, T. L., Mitjans, F., Piulats, J., Montgomery, A. M. P., Cheresh, D. A., and Brooks, P. C. Integrin $\alpha_V\beta_3$ promotes M21 melanoma growth in human skin by regulating tumor cell survival. Cancer Res., *59:* 2724–2730, 1999.

25. Castel, S., Pagan, R., Garcia, R., Casaroli-Marano, R. P., Reina, M., Mitjans, F., Piulats, J., and Vilaro, S. α_V integrin antagonists induce the disassembly of focal contacts in melanoma cells. Eur. J. Cell Biol., *79:* 502–512, 2000.

26. Scott, G. A., Liang, H., and Cassidy, L. L. Development of regulation of focal contact protein expression in human melanocytes. Pigm. Cell Res., *8:* 221–228, 1995.

27. Scott, G., Cassidy, L., and Busacco, A. Fibronectin suppresses apoptosis in normal human melanocyte through an integrin-dependent mechanism. J. Investig. Dermatol., *108:* 147–153, 1997.

28. Owen, C. S., Pooler, P. M., Wahl, M. L., Bobyock, S. B., Coss, R. A., and Leeper, D. B. Altered proton extrusion in cells adapted to growth at low extracellular pH. J. Cell. Physiol., *173:* 397–405, 1997.

29. Wahl, M. L., Bobyock, S. B., Leeper, D. B., and Owen, C. S. Effects of 42°C hyperthermia on intracellular pH in ovarian carcinoma cells during acute acidification or chronic exposure to low extracellular pH. Int. J. Radiat. Oncol. Biol. Phys., *39:* 205–212, 1997.

30. Wahl, M. L., Coss, R. A., Bobyock, S. B., Leeper, D. B., and Owen, C. S. Thermotolerance and intracellular pH in two Chinese hamster cell lines adapted to growth at low pH. J. Cell. Physiol., *166:* 438–445, 1996.

31. Owen, C. S., Wahl, M. L., Leeper, D. B., Perry, H. D., Bobyock, S. B., Russel, M., and Woodward, W. Accurate whole Spectrum measurements of intracellular pH and $[Na^+]$. J. Fluoresc., *5:* 329–335, 1995.

32. Moolenaar, W. H., Tsien, R. Y., vander Saag, P. T., and de Laat, S. W. Na^+/H^+ exchange and cytoplasmic pH in the action of growth factors in human fibroblasts. Nature (Lond.), *304:* 645–648, 1983.

33. Schwartz, M. A., Lechene, C., and Ingber, D. E. Insoluble fibronectin activates the Na^+/H^+ antiporter by clustering and immobilizing integrin $\alpha_V\beta_1$, independent of cell shape. Proc. Natl. Acad. Sci. USA, *88:* 7849–7853, 1991.

34. Schwartz, M. A., Ingber, D. E., Lawrence, M., Springer, T. A., and Lechene, C. Multiple integrins share the ability to induce elevation of intracellular pH. Exp. Cell Res., *195:* 533–535, 1991.

35. Grynkiewicz, G., Poenie, M., and Tsien, R. Y. A new generation of Ca^{2+} indicators with greatly improved fluorescence properties. J. Biol. Chem., *260:* 3440–3450, 1985.

36. Owen, C. S., Carango, P., Grammer, S., Bobyock, S., and Leeper, D. B. pH-dependent intracellular quenching of the indicator C-SNARF-1. J. Fluoresc., *2:* 75–80, 1992.

37. Popov, E., Gavrilov, I., Pozin, E., and Gabbasov, Z. Multiwavelength method for measuring concentration of free cytosolic calcium using the fluorescent probe Indo-1. Arch. Biochem. Biophys., *261:* 91–96, 1988.

38. Poole, R. C., and Halestrap, A. P. Transport of lactate and other monocarboxylates across mammalian plasma membranes. Am. J. Physiol., *264:* C761–C782, 1993.

39. Rosenberg, S., Fadil, T., and Schuster, V. A basolateral lactate/H^+ cotransporter in Madin-Darby canine kidney (MDCK) cells. Biochem. J., *289:* 263–268, 1993.

40. Owen, C. S., Wahl, M. L., Pooler, P. M., Coss, R. A., and Leeper, D. B. Temporal association between alterations in proton extrusion and low pH adaptation. Int. J. Hyperthermia., *14:* 227–232, 1998.

41. Roos, A., and Boron, W. Intracellular pH. Physiol. Rev., *61:* 296–434, 1981.

42. Burd, R., Wachsberger, P. R., Biaglow, J. E., Wahl, M. L., and Leeper, D. B. Absence of Crabtree effect in human melanoma cells adapted to growth at low pH: reversal by respiratory inhibitors. Cancer Res., *61:* 5630–5635, 2001.

43. Poole, R., and Halestrap, A. P. Reversible and irreversible inhibition, by stilbenedisulfphonates, of lactate transport into erythrocytes. Biochem. J., *275:* 307–312, 1991.

44. Briand, P., Peterson, O. W., and Van Deurs, B. A new diploid nontumorigenic human breast epithelial cell line isolated and propagated in chemically defined medium. In Vitro Cell. Dev. Biol., *23:* 181–188, 1987.

45. Martinez-Zaguilan, R., Martinez, G. M., Gomez, A., Hendrix, M. J., and Gillies, R. J. Distinct regulation of pH_{in} and $[Ca^{2+}]_{in}$ in human melanoma cells with different metastatic potential. J. Cell. Physiol., *176:* 196–205, 1998.

46. Warburg, O. The metabolism of tumours: investigations from the Kaiser Wilhelm Institute for Biology, Berlin-Dahlem., Vol. 40s., p. 327, 1930.

47. Ingber, D. E., Prusty, D., Frangioni, J. V., Cragoe, E. J., Lechene, C., and Schwartz, M. A. Control of intracellular pH and growth by fibronectin in capillary endothelial cells. J. Cell Biol., *110:* 1803–1811, 1990.

48. Sardet, C., Counillon, L., Franchi, A., and Pouyssegur, J. Growth factors induce phosphorylation of the Na^+/H^+ antiporter, a glycoprotein of 110 kD. Science (Wash. DC), *247:* 723–726, 1990.

49. Shuldiner, S., and Rozengurt, E. Na^+/H^+ antiport in Swiss 3T3 cells: mitogenic stimulation leads to cytoplasmic alkalinization. Proc. Natl. Acad. Sci. USA, *79:* 7778–7782, 1982.

50. Grinstein, S., Woodside, M., Waddell, T. K., Downey, G. P., Orlowski, J., Pouyssegur, J., Wong, D. C. P., and Foskett, J. K. Focal localization of the NHE-1 isoform of the Na^+/H^+ antiport: assessment of effect on intracellular pH. EMBO J., *12:* 5209–5218, 1993.

51. Raghunand, N., and Gillies, R. J. pH and drug resistance in tumors. Drug Resist. Updat., *3:* 39–47, 2000.

52. Schwartz, M. A. Signaling by integrins: implications for tumorigenesis. Cancer Res., *53:* 1503–1506, 1993.

53. Kroeger, M., Walenta, S., Rofstad, E. K., and Mueller-Klieser, W. Growth rates or radiobiological hypoxia are not correlated with local metabolite content in human melanoma xenografts with similar vascular network. Br. J. Cancer, *72:* 912–916, 1995.

54. Rofstad, E. K. Radiation sensitivity *in vitro* of primary tumors and metastatic lesions of malignant melanoma. Cancer Res., *52:* 4453–4457, 1992.

55. Spencer, T. L., and Lehninger, A. L. L-Lactate transport in Ehrlich ascites tumour cells. Biochem. J., *154:* 405–414, 1976.

56. Kim, J. H., Kim, S. H., Alfieri, A. A., and Young, C. W. Quercetin, an inhibitor of lactate transport and a hyperthermic sensitizer of HeLa cells. Cancer Res., *44:* 102–106, 1984.

57. Lin, R-Y., Vera, J. C., Chaganti, R. S. K., and Golde, D. W. Human monocarboxylate transporter 2 (MCT2) is a high affinity pyruvate transporter. J. Biol. Chem., *273:* 28959–28965, 1998.

58. Wilson, M. C., Jackson, V. N., Heddle, C., Price, N. T., Pilegaard, H., Juel, C., Bonen, A., Montgomery, I., Hutter, O. F., and Halestrap, A. P. Lactic acid efflux from white skeletal muscle is catalyzed by the monocarboxylate transporter isoform MCT3. J. Biol. Chem., *273:* 15920–15926, 1998.

59. Wang, X., Levi, A. J., and Halestrap, A. P. Substrate and inhibitor specificities of the monocarboxylate transporters of single rat heart cells. Am. J. Physiol., *270:* H476–H484, 1996.

Molecular Cancer Therapeutics

Regulation of Intracellular pH in Human Melanoma: Potential Therapeutic Implications 1 Supported by NIH Grant P01 CA56690 (to M. L. W., R. B., C. S. O., D. B. L.); Grant R25CA48010 from National Cancer Institute, NIH, and Department of Health and Human Services, National Science Foundation MCB RUI Grant 9057010 (to J. A. O., S. S. N., R. A. H.); and NIH Grant CA39248 (to D. B.). 1

Miriam L. Wahl, Judith A. Owen, Randy Burd, et al.

Mol Cancer Ther 2002;1:617-628.